Experimental assessment of cycling ageing of lithium-ion second-life batteries from electric vehicles

Elisa Braco, Idoia San Martín, Alberto Berrueta, Pablo Sanchis, Alfredo Ursúa (*)

Affiliation: Department of Electrical, Electronic and Communications Engineering, Institute of Smart Cities, Public University of Navarre, Campus de Arrosadia, 31006 Pamplona, Spain

(*) Corresponding author. Email address: alfredo.ursua@unavarra.es (A. Ursúa)

***Abstract* —** The reutilization of batteries from electric vehicles allows to benefit from their remaining energy capacity and to increase their lifespan. The applications considered for the second life of these batteries are less demanding than electric vehicles regarding power and energy density. However, there is still some uncertainty regarding the technical and economic viability of these systems. In this context, the study of the ageing and lifetime of reused batteries is key to contribute to their development. This paper assesses the experimental cycle ageing of lithium-ion modules from different Nissan Leaf through accelerated cycling tests on their second life. The evolution of the internal parameters during ageing and the correlation between them are shown, including the analysis of best fitting curves. In addition, a second-life end-of-life criterion is proposed, based on capacity and internal resistance measurements during cells ageing, which can be applied to real application in order to prevent safety issues. By estimating future values from degradation trends and checking latter measurements, the ageing knee is identified. Results show that the modules operate for at least 2033 equivalent full cycles before reaching their ageing knee. This would mean more than 5 years of operation in a real second-life application, such as a photovoltaic self-consumption installation with daily cycling. Moreover, it is shown that a traditional cell characterisation based on capacity and internal resistance measurements is not enough to predict the durability of a cell during its second life.

Keywords — Cycle ageing, Energy storage, Electric vehicle, Lithium-ion battery, Renewable energy, Second-life battery

1. Introduction

In recent years, environmental problems caused by traditional combustion vehicles have brought to a transition in the mobility sector towards electric vehicles (EVs) as a sustainable alternative. In 2018 the global stock of EVs exceeded 5.1 million worldwide, and it is foreseen that in 2030 there will be 130 million of EVs on our roads [1]. The expansion of the EV has a direct impact on the energy storage industry. Thus, the demand for lithium-ion batteries (LIBs) for EVs is expected to reach 1293 GWh in 2030 [2].

Automotive standards establish that LIBs must be retired from EVs when their capacity falls below 70 % to 80 % of the initial value [3,4]. Once they are discarded from EVs, LIBs are normally recycled. However, reutilization emerges as an alternative that allows to extend their useful life. In this context, the term First Life (FL) is applied to their use as energy storage in the EVs, whereas the term Second Life (SL) refers to their reutilization stage. The potential SL applications for these batteries are mainly stationary, with less demanding operating profiles than in their FL, and in which volumetric and gravimetric power and energy density are not as critical as in EVs. According to a report published by the European Commission, one of the most promising SL applications is energy storage in photovoltaic installations at residential level [5]. The reuse of EV batteries has aroused industrial and research interest in the last few years [6–8]. On the one hand, from the industrial point of view, the potential of SL batteries is especially interesting for automotive companies such as Nissan [9], BMW [10] or Daimler [11], which, in partnership with energy companies, have built large-scale demonstrators. On the other hand, several aspects have been analysed by means of research projects and contributions, namely environmental benefits [12–14], situation of policies and market [15] or hardware and control adapted to SL systems [16,17]. However, the main focuses of SL LIBs research are economical and technical viability.

Regarding economic assessments of reused batteries, some authors are optimistic about their profitability [18–20], while others stress the relevance of the battery cost for its financial return [21,22], which leads to a thorough monitoring of the evolution of this market [23]. Moreover, the economic benefits of reused batteries in renewable energy systems, such as wind farms, may be compromised by other factors, including wind prices and the price gap between new and SL batteries [24]. In what EV LIB concerns, their economic viability is highly influenced by their performance and durability. Therefore, several technical studies concerning these two issues have been recently published.

From one side, several technical contributions regarding SL battery performance have been reported from different perspectives. The first approach is the use of simulation tools, which employ mathematical and physical models to analyse battery operation. These studies have found feasible scenarios for SL LIBs, such as isolated microgrids, solar energy integration or transportation and grid services [25–27]. A key factor pointed out by simulation research to reduce SL cells performance and durability is the dispersion of the internal parameters (mainly capacity and internal resistance) [28], due to the limitations imposed by the required serial connection of the cells in battery packs. Therefore, the quantification of cell dispersion [29] and proper reconfiguration [30] have been analysed in order to improve the performance of SL LIBs. Besides simulation studies, several experimental contributions have evaluated the operation of reused LIBs in different applications. These investigations cover technical aspects related to battery control and management in various implementations with different storage power and energy requirements. SL LIBs have been proved to be a feasible energy storage system for applications ranging from high power specifications, such as frequency regulation services [31], to high energy requirements, namely energy time shifting and demand side management at residential scale [32,33]. Moreover, the stacking of various services, which enhances the profitability of the battery, has been proved to be a feasible application for SL LIBs. The combination high-power and high-energy services, such as frequency regulation and peak shaving [34] or power smoothing and residential energy requirements [35], is the most interesting approach for these batteries.

However, a technical study is not enough to guarantee the safe performance of a SL LIB, given the relevant changes in the characteristics of its cells as a result of ageing. Due to the degradation mechanisms that take place in a cell, its energy and power capabilities fade. This can be quantified from its capacity loss and internal resistance rise. During most of a LIB lifetime, capacity fade and resistance rise rates are constant, given that its main degradation mechanisms remain unchanged. However, at a certain point during battery life, new ageing mechanisms become more relevant, especially lithium plating [36,37], thereby increasing the battery ageing rate. This point is named ageing knee, and is related to a change of trend in capacity and resistance evolution [38]. The operation of LIBs beyond the ageing knee involves safety risks, such as increased chances of internal short circuits [36,39]. From the point of view of EV manufacturers, the ageing knee is not a critical concern, given that the battery is discarded beforehand as it cannot meet the autonomy requirements of the vehicle. However, the identification of this turning point becomes crucial in SL applications, in which the battery is worn out up to its safety limit. Despite several studies having analysed the nonlinear performance of LIBs, most of them are focused on non-automotive cells, which are aged by means of accelerated tests in order to reach the ageing knee [37,38,40]. Only Martinez-Laserna et al. [35] assess the nonlinear performance of automotive cells, even though the samples do not come from actual EVs, but are artificially aged by means of accelerated tests from the beginning of their first life.

An overall ageing characterisation of reused lithium-ion cells extracted from actual EVs covering the whole second life, including the ageing knee, would provide critical and trustworthy information for a proper analysis of such energy storage systems, and therefore would be a powerful tool for the analysis of second-life batteries feasibility. The aim of this paper is to shed light on this full second-life ageing characterisation. Specifically, six modules extracted from different Nissan Leaf EVs are cycled, with periodical measurements of their capacity and internal resistance. These results are shown in detail, along with an analysis of the evolution of the main parameters and their correlation.

The remaining sections of this paper are organised as follows. Section II describes the tested modules and the experimental procedure. Section III shows the experimental results, with special regard to the evolution of parameters and their correlation during ageing. Section IV presents a discussion of the results, highlighting the most remarkable contributions to the state of the art and, finally, Section V summarises the findings and states the main conclusions.

2. Experimental setup

2.1. Module description

The experimental part of this contribution has been carried out with six modules from different Nissan Leaf EVs (see Fig. 1a), whose FL history is unknown, given that the company does not provide such information nowadays. Each module consists of four pouch cells with manganese oxide and graphite electrodes (LMO/C). As shown in Fig. 1b), these four cells are connected in a 2s2p assembly. Each module has three external terminals: positive (R), middle point (W) and negative (B). Therefore, it is not possible to access the cells individually, but in 2p pairs. Given that these 2p pairs are the smallest unit available, and in order to improve readability, they will be hereafter named as cell. The main specifications of cell and module are shown in Table 1. Note that the mass of the cells represents 82 % of the global mass of the module, as stated in the last row of the table. This variable is especially interesting for the calculation of the specific energy of the cells.

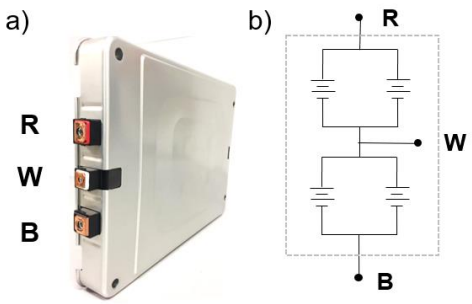

Fig. 1. a) Picture and b) electrical schematic of a Nissan Leaf module. A half of each module (two parallel-connected cells) is tested in this paper. This structure will be called cell for improved readability.

	Module	**Cell (2p)**
Nominal Voltage (V)	7.50	3.75
Maximum Voltage (V)	8.30	4.15
Minimum Voltage (V)	5.0	2.5
Rated Capacity (Ah)	66	66
Rated Energy (Wh)	495.0	247.5
Length x Width x Thickness	303 mm x 223 mm x 35 mm	-
Mass (g)	3850	1574

Table 1. Module and cell specifications.

2.2. Experimental procedure description

In order to assess the durability of reused cells from EVs, an accelerated cycling profile is chosen. The test consists of a sequence of full charge and discharge cycles between the voltage limits of the cell. The charging method is Constant Current – Constant Voltage (CC-CV), with a cut-off current of C/20, while the discharging procedure is CC. The current applied on the CC stages is 1C. The C-rate is defined based on the rated capacity of the cell at the beginning of its FL. All the tests are performed on the positive 2p cell in a controlled environment of 25 °C.

Every 25 cycles each cell is subjected to a Reference Performance Test (RPT), in order to characterise the degradation due to their ageing. Each RPT comprises a capacity and internal resistance test, executed sequentially. The capacity test consists of two full cycles with CC-CV charge and CC discharge until the maximum and minimum cell voltage respectively. The CC stage current is C/3 and the cut-off current is C/33. The capacity measured on the discharge of the second cycle is considered as the current cell capacity (C_A). Furthermore, the Direct Current Internal Resistance (DCIR) is measured from discharge pulses at different State of Charge (SOC) levels. The test starts with a complete CC-CV charge at C/2 with C/20 as cut-off current. Then, a CC discharge pulse of C/2 is performed, until the cell reaches 90 % of SOC. After a rest period of 1 hour, the cell is discharged with a CC pulse at C/2 until the next SOC level. This procedure is repeated for SOC levels of 70 %, 50 %, 30 % and 10 %. The DCIR at each SOC is measured after 10 seconds of discharge pulse. Fig. 2 shows 10 cycles of the accelerated cycling profile and an RPT from an experimental sequence of one of the ageing tests of this contribution. The voltage measured in the 2p cell is shown in the left Y axis, whereas the right Y axis corresponds to the test current.

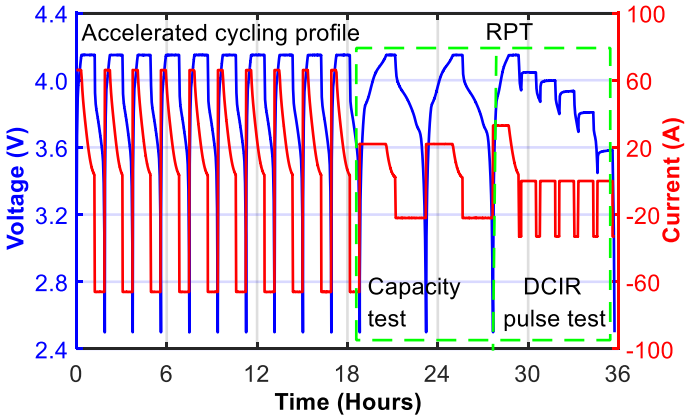

Fig. 2. Evolution of voltage and current on a cell during 10 cycles of accelerated profile and an RPT.

The test bench consists of two battery cyclers of 16 channels (5 V and 50 A each), with an accuracy of ±0.1 % of the full scale, and a thermal chamber (temperature range -30 ºC to +180 ºC), which has a temperature accuracy of ±0.5 ºC.

A critical aspect of the experimental procedure of this contribution is the definition of the End of Test (EOT). As it is aimed to identify the ageing knee of the cells, the tests will cover their linear and nonlinear performance. Given the fair risk of sudden failure after the ageing knee, two stop criteria are set for the tests. The first criterion is related to capacity evolution and it aims to identify sudden losses. This criterion is fulfilled if capacity fades more than 6 % of the rated value over 100 sequential cycles. The second criterion is focused on extremely low capacity values, and it is fulfilled when capacity decreases below a 30 % of the rated value. If any of the stop criteria is met, the experiment is immediately interrupted.

3. Results

The six Nissan Leaf cells were tested according to the accelerated cycling profile. After 13 months of test, only one of the samples, M5, has not fulfilled any of the EOT criteria. This section presents the experimental results of the tests, focusing on the evolution of the main parameters during ageing and the correlation between them.

3.1 Evolution of the main parameters

The prolonged ageing test of this contribution allows to characterise cell degradation in depth, covering the ageing knee and therefore providing interesting information of SL performance. This first subsection is focused on the experimental evolution of the main parameters, namely capacity and internal resistance throughout time. As a complete indicator of cell performance, the evolution of the energy delivered by the cells will also be shown.

3.1.1 Capacity

Capacity tracking during SL performance is of great interest in view of the identification of the different ageing stages. Fig. 3 shows the experimental results of capacity measurements from the RPTs for the 6 SL cells tested in this contribution. The X axis represents the total number of cycles of the test.

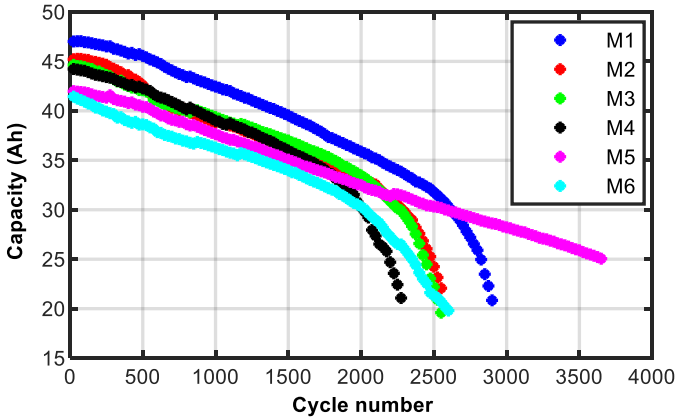

Fig. 3. Evolution of capacity measurements from the RPTs vs. cycle number on the 6 SL cells tested.

As it can be seen in the figure, the initial capacity values measured in the first RPT ($C_{RPT(1)}$), vary from 41.4 Ah to 47.0 Ah, which correspond to State of Health (SOH) values of between 62.8 % and 71.2 %. The SOH is computed as the ratio between the actual capacity of the cell (C_A), and the rated capacity (C_R), which is provided in Table 1. Thereby, $SOH=C_A/C_R$. On the other hand, the capacity fade of a given module is computed considering the initial value of the test and the actual capacity at a certain RPT, through the expression $C_{FADE}= (C_{RPT(1)}-C_A)/C_{(RPT(1)}$. In the initial stages of the test, capacity decreases with a linear trend in all the cells during at least 1850 cycles. The average slope of this phase is -5.75 mAh per cycle. An increasing slope of the capacity loss rate indicates the beginning of the ageing knee. The turning point is observed in five out of six cells after between 1875 and 2520 cycles. The SOH of the cells in the ageing knee varies from 45 % to 49.5 %, the capacity fade since the beginning of the test is between 26 % and 33 %. Regarding the nonlinear evolution of capacity, a quadratic polynomial offers a good fitting for the curve, with an average R^2 of 0.996. It is remarkable that M5 continues with a linear capacity fade after 3650 cycles, with a SOH of 38 %. This cell has lost at this point 40 % of its capacity from the beginning of the SL test.

Note that the EOT criteria described in Section 2 are fulfilled in five of the modules after between 2275 and 3175 cycles. The SOH measured at this point ranges from 24 % to 33 %. Considering the capacity fade from the beginning of the SL test, the least aged cell at its EOT is M2, with 51 % of capacity loss after 2550 test cycles. Conversely, M3 presents a capacity fade of 56 % after the same number of cycles.

3.1.2 Internal Resistance

In this subsection the evolution of the internal resistance of the cells as a result of cycle ageing is examined. Given that the ageing trends are similar for the DCIR pulse measurements in all the SOC levels of the RPT test, the measurements at *SOC* = 50 % are shown as a reference for the study. Fig. 4 depicts these DCIR measurements, with the total number of cycles represented in the X axis.

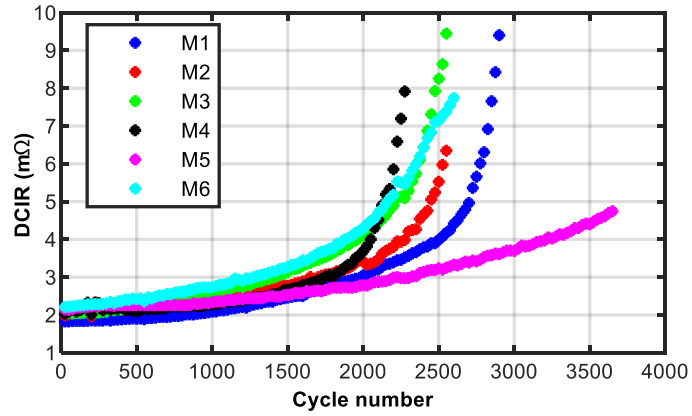

Fig. 4. Evolution of the DCIR measurements from the RPTs at 50% of SOC vs. cycle number on the 6 SL cells tested.

As the figure shows, DCIR follows a linear trend at the beginning of the test. However, as the module ages, the resistance rise becomes nonlinear, and eventually there is a sharp increase of this parameter. The average slope of the linear stage is 22.4 μΩ per cycle. After between 1250 and 2075 cycles a turning point

is observed in this parameter, and its increase rate becomes nonlinear. Considering the nonlinear part of the curve, the most suitable fitting for the evolution of DCIR is a cubic polynomial, which offers an average R^2 of 0.9873.

Given that the FL nominal value of DCIR is not provided by the manufacturer, it is not possible to quantify the resistance rise related to the brand-new battery. Therefore, the results obtained in this parameter can only be related to the initial SL test measurement. Thus, it is found that the resistance rise at the ageing knee is between 60 % and 123 % of the initial value. Additionally, at the EOT point, the values of DCIR have risen from 219 % to 414 % compared to the initial RPT. Note that M5 continues cycling, not having reached the ageing knee, and presents a DCIR rise of 121 % of the initial RPT after 3650 cycles.

3.1.3 Energy

In order to evaluate the real performance of the SL cells, the evolution of the energy delivered is analysed in this subsection. Fig. 5 shows in the left Y axis the evolution of the discharged energy measured in the second cycle of the capacity RPTs for the 6 SL cells of this work. The X axis presents the cycle numbers of each RPT.

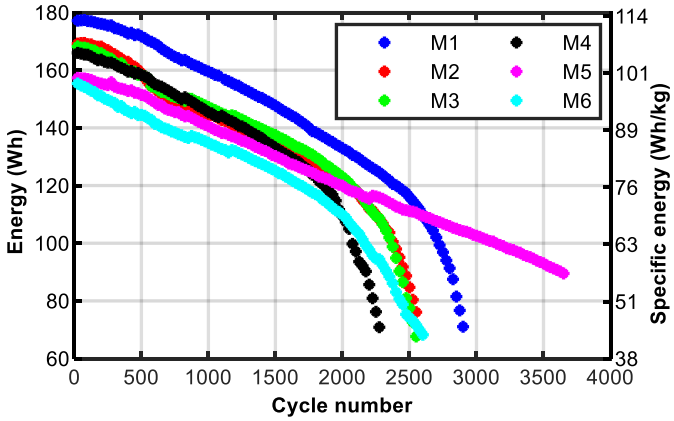

Fig. 5. Evolution of the energy measurements from the RPT (left axis) and specific energy at cell level (right axis) vs. cycle number on the 6 SL cells tested

As it can be seen in the figure, the discharge energy fades with a linear trend until a certain point, from which it suffers a sudden loss and becomes nonlinear. The average slope of the linear stage is -10.4 mWh per cycle. Five out of the six cells reach the ageing knee after between 1875 and 2500 cycles. The values of discharge energy measurements related to the nominal value range from 43 % to 48 %. Considering the energy lost in the modules since the beginning of the SL test, there is a fade between 28 % and 34 %. On the other hand, at the EOT the cells deliver from 22 % to 31 % of the nominal energy. Considering the whole evolution on the SL test, there is an energy fade of between 55 % and 65 %. For its part, the module M5 delivers 36 % of the nominal energy after 3650 cycles, having lost 43 % of energy from the beginning of the SL test.

An interesting aspect from the point of view of the application is the energy density of the cells. Fig. 5 shows, in the right Y axis, the specific energy of the cell. As it can be seen, throughout the SL test the values vary between 113 Wh/kg and 43 Wh/kg. Considering the rated values of Table 1, the specific energy of a brand-new cell is 157.24 Wh/kg. Hence, the energy density on the SL test varies from 72 % to 27 %.

3.2 Correlation between parameters

Besides the evolution of each internal parameter of a cell, another interesting approach is the analysis of their correlation along the various ageing stages. Given that this experimental contribution covers SL cells performance before and after the ageing knee, the influence of the different ageing phases on the correlation between the internal characteristics of a cell is examined in this subsection.

3.2.1 Capacity and internal resistance

Capacity and internal resistance are the main parameters of a lithium-ion cell. Being directly related to the energy and power capabilities of the cell, their correlation during ageing is key to assess cell performance. Fig. 6 presents the evolution of capacity and DCIR measurements from the RPT carried out on the 6 SL cells over the whole cycle ageing test.

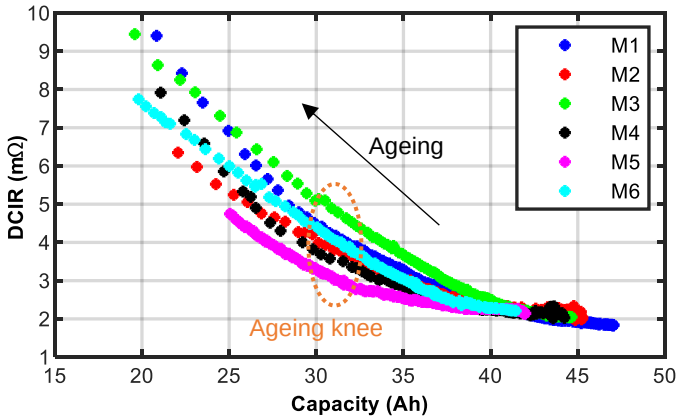

Fig. 6. Evolution of the DCIR measurements from the RPT at 50% of SOC vs. capacity of the 6 SL cells tested.

As the figure shows, high capacity values correspond to low measurements of DCIR, which are related to early stages of ageing. As capacity decreases, DCIR measurements increase, therefore indicating a higher degradation degree and more advanced ageing phases. In order to determine the best fit for the data, lineal and second-degree polynomial expressions are analysed. The correlation is found to be nonlinear, and quadratic polynomials offer good fittings for these curves, being the average R^2 = 0.995. Note that no change of trend is observed after the ageing knee.

3.2.2 Capacity and energy

Even though capacity is generally associated with the energy stored in a cell, it is interesting to analyse how prolonged ageing affects the correlation between capacity and energy capabilities. Fig. 7a) shows the measurements of discharge energy (E_{dch}) vs. capacity (C) of the RPTs on the 6 SL cells tested. As it can be seen in the figure, the correlation between these parameters is linear during all the SL tests. Hence, the change of trend in capacity associated with advanced states of ageing has a direct correspondence with the energy delivered. The evolution of the ratio between these parameters, namely the average discharge voltage ($V_{dch} = E_{dch} / C$) is plotted in Fig. 7b). As it is shown in the figure, despite being similar to the nominal voltage value (3.75 V) in the early stages of the test, the discharge voltage decreases as cells age. This reduction is linear at the beginning of the test, but it is accelerated on a second step. It is noteworthy that the ageing knee is observed in the discharge voltage of the cell, while the relationship between capacity and energy remains linear during the whole test.

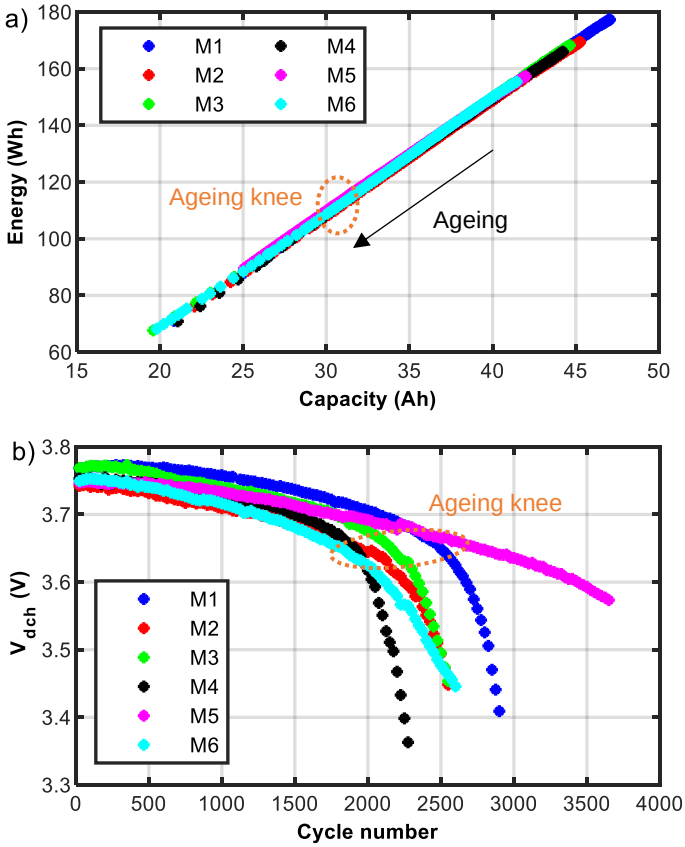

Fig. 7. a) Evolution of discharge energy vs. capacity measurements on the RPTs and b) average discharge voltage vs. cycle number of the 6 SL cells tested.

3.2.3 Internal resistance and energy

In this contribution, the performance limits regarding cells discharge are related to voltage, being therefore influenced by their internal resistance. As stated previously, the internal resistance of the SL cells suffer a change of trend in advanced stages of ageing. However, this occurs before the ageing knee, and therefore prior to the turning point of capacity evolution. Hence, it is interesting to analyse separately how DCIR affects the energy delivered by the cells during their ageing. Fig. 8 depicts the discharge energy vs. the DCIR measurements at 50% of SOC on the RPTs throughout the cycle ageing test.

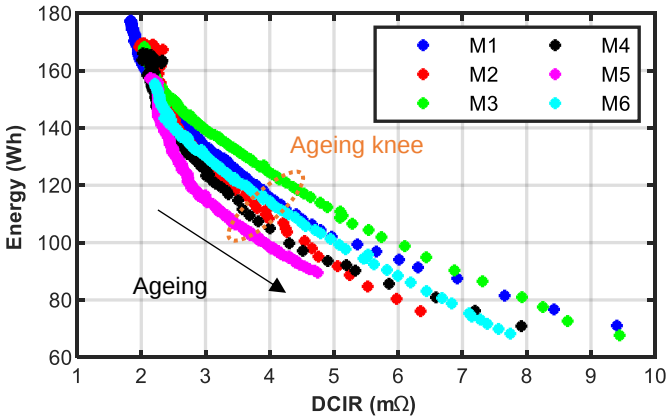

Fig. 8. Evolution of discharge energy vs. DCIR measurements on the RPTs of the 6 SL cells tested.

As the figure shows, the correlations between DCIR and energy delivered by the cells are nonlinear during all the SL tests. Unlike the separate evolution of these parameters through ageing, no change of trend is identified. Cubic polynomial expressions offer good fittings for these correlations, providing an average R^2 of 0.984.

4. Discussion and contributions

From the literature review presented in Section 1, a gap in the technical assessment of reused cells from EVs was identified. While most of the previous research of cycle ageing of SL LIBs focus on the performance before the ageing knee [41–43],the contributions which include nonlinear behaviour of the cells do not analyse samples from real EVs [35].In this context, this work presents the experimental results of 13 months of experimental cycling on six reused cells retired from real EVs. In this section, the main findings of this contribution are discussed.

4.1 Characterisation of cell degradation

From the point of view of SL cell performance, it is interesting to analyse how it is affected by the degradation of the internal parameters, and which aspects are the most worsened. The characterisation of the 6 SL cells during the ageing test presented in Section 3 shows that both capacity and internal resistance suffer a change of trend in advanced stages of ageing. However, this turning point appears before in DCIR, and, along with the faster degradation of this parameter, leads to a nonlinear correlation between capacity and internal resistance in the SL cells. In terms of cell performance, it is found that the relationship between discharge energy and capacity is linear during all the test. It can be thus assumed that capacity is a good indicator of the energy capabilities of the cell even after the ageing knee. Furthermore, the influence of the internal resistance on the discharge energy is also examined in Section 3. On the one hand, it is shown that the average discharge voltage, computed as the ratio between discharge energy and capacity, suffers a change of trend during ageing. Despite being similar to the nominal voltage at the beginning of the test, it suffers a sudden decrease in advanced stages of ageing, which is related to the sharp increase of the internal resistance. Given that the discharge performance of the SL tests of this contribution is determined by a voltage limit, the degradation of the internal resistance leads to a faster threshold achieving. On the other hand, the influence of this parameter on the energy delivered is confirmed by the cubic correlation observed during all the SL test. Hence, it can be assumed that during the SL of a lithium-ion cell, the combination of both internal resistance rise and capacity fade aggravates the energy loss.

A further point of discussion is the comparison of the evolution trends between SL cells. Unlike their fresh homologues, retired cells from EVs may present very different ageing states at the beginning of their performance. Therefore, it is of great interest to analyse the degradation of their various parameters during ageing. As presented in Section 3, capacity shows a similar trend on five of the cells tested and becomes nonlinear in the ageing knee. Similarly, the DCIR of the cells increases linearly in the early stages of the SL test, then it becomes nonlinear and finally suffers a sharp rise after the ageing knee. Nevertheless, the number of cycles performed until this turning point varies from 1875 to 2550. These differences on the ageing rates could be related to the FL history of the modules [41]. As in this work the FL data is unknown, it is not possible to determine whether the start of the knee corresponds to a similar number of equivalent cycles from the beginning of the modules FL.

Moreover, it is intriguing to study the evolution of the internal parameters of the cell according to their initial SL state. For instance, M5 and M6 have similar SOH (63.6 % and 62.7 %) and DCIR (2.15 mΩ and 2.21 mΩ) at the beginning of the SL test. However, M6 shows an acceleration on capacity fade after 2050 cycles, while M5 has performed during 3650 cycles with no sign of the ageing knee. Even M1, the cell the least aged at the beginning of the SL test, with a capacity of 71 % of a brand-new battery and an internal resistance of 1.83 mΩ, has reached the ageing knee after 3525 cycles. Therefore, it can be stated that traditional measurements of capacity and internal resistance, such as the ones performed in this article, are not enough to predict the performance of the cells during their SL.

4.2 Ageing knee identification

While the retirement point of LIB in EVs is defined by automotive standards based on a SOH level, the end of life at their SL is not yet clearly defined. Some authors stablish also a SOH level as retirement criteria [14,27], whereas others suggest that it should be defined when capacity fade rate changes from linear to nonlinear, in the so-called ageing knee [35]. The identification of the retirement point for SL batteries is key to ensure a safe operation of the modules, and it plays an important role on the economic viability of these systems.

In this context, this contribution explores the identification of the ageing knee, and proposes a criterion to define it from experimental measurements. The basis of the ageing knee is the acceleration of the capacity fade rate of the cells. As starting hypothesis, it is assumed that the SL cells have not reached the ageing knee at the beginning of the test. From the capacity values measured on the RPTs, a linear expression of capacity as a function of the cycle number can be set. This expression allows to estimate capacity values of future RPTs, and to detect if real measurements of these RPTs correspond with the predictions. During the experiment, outlier measurements could also lead to an important estimation error. Hence, enough cycles

for the predicted RPT value should be set to ensure that the point corresponds to a real change of trend. On the other hand, the maximum estimation error should be chosen so that the ageing knee is identified accurately. In this work, for a given RPT, the linear equation is computed from the 500 previous cycles and the value of the RPT corresponding to the next 100 cycles is estimated. The threshold estimation error that indicates the ageing knee is set to 3 %.

From the ageing knee definition proposed, the turning point is detected in five of the cells tested after between 1875 and 2550 cycles. The SOH levels of the cells at this point ranges from 45 % to 49.5 %, while the capacity fade of the modules from the beginning of the test is between 26 % and 33 %. Even though the SOH or capacity fade could provide an estimation for the apparition of the ageing knee, the selection of these variables as SL retirement criteria would be less accurate and could underestimate the possibilities of the SL cells. The performance of M5 is a good example, as it continues the SL test showing a linear capacity fade trend with a SOH of 38 % and a capacity loss of 40 %.

As already mentioned, the ageing knee is mainly associated to lithium plating as additional ageing mechanism on the cells. Thereby, the capacity fade rate changes from linear to nonlinear at this point. Although the evolution of the internal resistance is already nonlinear in the ageing knee, a sharp rise of this parameter is also detected. Hence, the proposed ageing knee identification procedure is also applied to the DCIR measurements of this contribution. Since the change rate of DCIR is greater than that of capacity, the threshold estimation error that indicates the ageing knee is set to 6 %. Results show that the ageing knee is identified by means of this method with a maximum deviation of 2.3 % with respect to the capacity results. Given that DCIR measurements are much simpler than capacity and less time-consuming, the identification of the ageing knee regarding this parameter could ease the end of life detection. However, it should be noted that resistance measurements are usually less accurate than capacity and, therefore, a suitable repeatability of measurements should be considered in order to ensure an accurate identification of the ageing knee. Since only capacity or internal resistance measurements are required in the proposed methodology, it can be generalised to real applications without standard cycling. Given that current pulses are usual in real scenarios, voltage and current tracking would be enough to determine the evolution of DCIR in the battery, thereby allowing the detectionof sharp rises in this parameter. Besides, the method does not depend on battery chemistry, and therefore it can be extended to other Li-ion batteries reused in SL applications.

4.3 Durability

The durability of SL LIBs is key for their economic viability. As stated before, the operation of these batteries should be restricted before they suffer an acceleration in the degradation rate, so that safety risks are avoided. In this context, this contribution proposes to relate the durability of the cells to the ageing knee. In order to estimate the real implications of the results obtained, the number of Equivalent Full Cycles (EFC) is computed, taking into account the charge throughput of the cells during the accelerated ageing cycles, as well as during the RPTs. Hence, five out of the six cells analysed in this work have performed between 2033 and 2748 EFC under the accelerated cycling profile before reaching the ageing knee. The sixth cell, M5, continues with a linear degradation rate after 3846 FEC.

It is noteworthy that the operating conditions of the cells play a key role on their performance and durability. Factors such as temperature, time, charge and discharge rates or depth of discharge are specific of each test and difficult the accurate extrapolation of the results. However, some estimations can be made regarding the implications on real SL applications.

In this context, the durability results presented in this paper are extended to one of the most promising applications for SL batteries: PV energy grid integration in residential applications. According to recent research work on this field [44], three cycling scenarios can be considered, as summarised in Table 2. The first case study is a mild cycling scenario, with one cycle every two days, which could correspond to a residential system with low solar generation or with an oversized storage system. Such oversizing of the battery is a typical situation in SL applications for instance in case of the direct reutilization of battery packs from EVs in residential facilities, given its simplicity and cost-effectiveness [32]. The second scenario corresponds to a domestic usage with an energy management strategy of maximum self-consumption, consisting of one cycle per day, with diurnal charges and nocturnal usage of the stored energy. Finally, the third case study considers stacked services at residential level, with an intensive cycling of 4 cycles per day, including energy services such as augmented self-consumption and bill management, as well as power services such as primary regulation and voltage support. Based on the experimental durability results of the six SL cells presented in this paper, Table 2 shows their estimated cycle lifetime according to the three scenarios described.

	Scenario	FECs per year	Cycle lifetime (years)
Residential	Mild cycling	183	11 – 21
	Maximum self-consumption	365	5.5 – 10.5
	Stacked services	1460	1.4 – 2.6

Table 2. Estimated cycle lifetime of SL cells on three PV residential scenarios.

As it can be seen in the table, mild cycling scenarios would lead to at least 11 years of cycle lifetime of the SL cells, while normal usage would imply between 5.5 and 10.5 years. This result agrees with previous experimental work with real profiles in SL cells [35], which predicts 4 years of operation in a typical residential application. If the SL cells were cycled intensively in stacked services, they would reach the ageing knee after 1.4 to 2.6 years of operation, a sensibly shorter lifetime due to the intensive usage of the energy storage system. These estimations provide a guide for further research on the economic viability of SL batteries.

It should be yet noted that the tests have been carried out under specific conditions of accelerated cycling and with a particular battery chemistry. Therefore, a deeper analysis on accurate ageing models of SL cells is highly recommended. Moreover, calendar ageing is not studied in this contribution, and the actual lifetime of SL batteries would be reduced due to this issue, especially in scenarios requiring a low use of the battery. On the other hand, the extrapolation of the results obtained to other battery chemistries should be carefully considered, given that each technology has its own particularities.

5. Conclusion

This contribution presents the experimental assessment of the durability of six SL cells from different Nissan Leaf electric vehicles, through accelerated cycling ageing tests.

Firstly, the degradation of the cells is characterised during ageing by tracking the evolution of their internal parameters. Both capacity and internal resistance (DCIR) show a linear trend at the initial stages of the second life test. The first change of slope is observed in DCIR, which becomes nonlinear with a cubic polynomial as best fitting curve. Conversely, the capacity fade becomes nonlinear with a quadratic polynomial trend. In terms of performance, capacity is stated to be a good indicator of the energy capabilities of the cells, as they are related linearly during all the SL stages. Moreover, it can be assumed that the degradation of both capacity and internal resistance affects negatively the energy delivered by the SL cells.

The prolonged cycle ageing through standard test of this contribution has enabled to characterise the complete evolution of the parameters, including the transition to the accelerated degradation stage. Hence, a stop criterion for the operation of SL cells is proposed. This criterion is based on capacity or internal resistance measurements. From previous test data, the values of future parameters are predicted, and latter checked with real values. If the estimation error is greater than 3 % in case of capacity or 6 % in case of DCIR, it is considered that the cell has reached the ageing knee and therefore the test should be interrupted. The simplicity of these measurements, especially the internal resistance, allows to have quick indicators for the identification of the ageing knee. Hence, the stop criterion for the operation of SL cells can be extended to real applications with specific profiles, no matter the specific Li-ion battery chemistry.

Moreover, the experiments presented in this paper show the durability of six SL lithium-ion cells. A safe performance of the cells inside the linear ageing region during at least 2033 EFC is shown. After more than 3846 EFC, one of the samples has not yet reached the ageing knee and continues with a linear capacity fade. Based on the capacity and DCIR measured at the beginning of the test, this cell could have been classified as one of the most aged among the samples. However, the experimental results show that it has the highest potential for SL applications. Therefore, we conclude from this study that traditional cell characterisation techniques based on capacity and DCIR measurements are not enough to predict the durability of a cell during its SL.

Finally, an estimation of the cycle lifetime of SL batteries used as energy storage for PV energy grid integration in residential applications is presented. The tested SL cells would perform more than 5 years under the most typical energy management strategy in residential systems, aimed at maximising the self-consumption rate. Additionally, two alternative scenarios have been studied: (i) an oversized battery or low PV generation subject to a milder cycling profile, which would last 11 to 21 years; and (ii) a domestic battery that also offers grid balancing services, which entails a harder cycling profile, thereby reducing its durability to less than 3 years. Note should be taken that the ageing tests have been performed under accelerated profile and with stable and favourable temperature conditions. Hence, it would be necessary to enlarge the testing matrix, develop accurate ageing models for SL batteries and run the cells under real application

profiles in order to enhance the accuracy of these results. On the other hand, the impact of calendar ageing is out of the scope of this contribution, and the actual lifetime of SL batteries would be reduced due to this issue, especially in scenarios requiring a low use of the battery. Moreover, the extrapolation of the results to other battery chemistries should be carefully considered, given that the particularities of each chemistry may influence them.

All in all, this contribution validates the technical viability of SL cells from EVs, showing a satisfactory cycling operation during at least 2033 equivalent full cycles. This technical potential of operation and durability should be accompanied by significantly lower costs than FL batteries, so that their integration in stationary applications will become a reality.

6. Acknowledgements

We would like to acknowledge the support of the European Union under the H2020 project STARDUST (774094), the Spanish State Research Agency (AEI) and FEDER--UE under grants DPI2016-80641-R, DPI2016-80642-R, PID2019-111262RB-I00 and PID2019-110956RB-I00, of Government of Navarra through research project 0011-1411-2018-000029 GERA and of Public University of Navarre under project ReBMS PJUPNA1904.

7. References

[1] International Energy Agency, Global EV Outlook 2019, Paris, 2019.

[2] C. Curry, Lithium-ion Battery Costs and Market, BNEF, 5 July 2017, (2017). https://data.bloomberglp.com/bnef/sites/14/2017/07/BNEF-Lithium-ion-battery-costs-and-market.pdf.

[3] IEC, IEC 62660 - 1: Secondary lithium-ion cells for the propulsion of electric road vehicles - Part 1: Performance testing, (2010).

[4] J.P. Christophersen, Battery Test Manual For Electric Vehicles, Revision 3, (2015). https://doi.org/10.2172/1186745.

[5] L. Boon-Brett, A. Pfrang, M. Messagie, F. Mathieux, A. Podias, F. Di Persio, A. Kriston, S. Bobba, Sustainability Assessment of Second Use Applications of Automotive Batteries: Ageing of Li-Ion Battery Cells in Automotive and Grid-Scale Applications, World Electr. Veh. J. 9 (2018) 24. https://doi.org/10.3390/wevj9020024.

[6] E. Martinez-Laserna, I. Gandiaga, E. Sarasketa-Zabala, J. Badeda, D.I. Stroe, M. Swierczynski, A. Goikoetxea, Battery second life: Hype, hope or reality? A critical review of the state of the art, Renew. Sustain. Energy Rev. 93 (2018) 701–718. https://doi.org/10.1016/j.rser.2018.04.035.

[7] E. Hossain, D. Murtaugh, J. Mody, H.M.R. Faruque, M.S.H. Sunny, N. Mohammad, A Comprehensive Review on Second-Life Batteries: Current State, Manufacturing Considerations, Applications, Impacts, Barriers Potential Solutions, Business Strategies, and Policies, IEEE Access. 7 (2019) 73215–73252. https://doi.org/10.1109/ACCESS.2019.2917859.

[8] R. Reinhardt, I. Christodoulou, S. Gassó-Domingo, B. Amante García, Towards sustainable business models for electric vehicle battery second use: A critical review, J. Environ. Manage. 245 (2019) 432–446. https://doi.org/10.1016/j.jenvman.2019.05.095.

[9] Nissan, Eaton, Energy storage for Buildings : designed and built for sustainability and resilience, (2017).

[10] B. Gohla-Neudecker, M. Bowler, S. Mohr, Battery 2nd life: Leveraging the sustainability potential of EVs and renewable energy grid integration, 5th Int. Conf. Clean Electr. Power Renew. Energy Resour. Impact, ICCEP 2015. (2015) 311–318. https://doi.org/10.1109/ICCEP.2015.7177641.

[11] Daimler AG, World's largest 2nd-use battery storage is starting up, (2016) 1–2.

[12] S. Bobba, F. Mathieux, F. Ardente, G.A. Blengini, M.A. Cusenza, A. Podias, A. Pfrang, Life Cycle Assessment of repurposed electric vehicle batteries: an adapted method based on modelling energy flows, J. Energy Storage. 19 (2018) 213–225. https://doi.org/10.1016/j.est.2018.07.008.

[13] M.A. Cusenza, F. Guarino, S. Longo, M. Ferraro, M. Cellura, Energy and environmental benefits of circular economy strategies: The case study of reusing used batteries from electric vehicles, J. Energy Storage. 25 (2019) 100845. https://doi.org/10.1016/j.est.2019.100845.

[14] L. Ahmadi, S.B. Young, M. Fowler, R.A. Fraser, M.A. Achachlouei, A cascaded life cycle: reuse of electric vehicle lithium-ion battery packs in energy storage systems, Int. J. Life Cycle Assess. 22 (2017) 111–124. https://doi.org/10.1007/s11367-015-0959-7.

[15] K. Gur, D. Chatzikyriakou, C. Baschet, M. Salomon, The reuse of electrified vehicle batteries as a means of integrating renewable energy into the European electricity grid: A policy and market analysis, Energy Policy. 113 (2018) 535–545. https://doi.org/10.1016/j.enpol.2017.11.002.

[16] M. Bauer, J. Wiesmeier, J. Lygeros, A comparison of system architectures for high-voltage electric vehicle batteries in stationary applications, J. Energy Storage. 19 (2018) 15–27. https://doi.org/10.1016/j.est.2018.06.007.

[17] S. Kratz, B. Krueger, R. Wegener, S. Soter, Integration of Photovoltaics into a Smart Trolley System Based on SiC-Technology, 2018 IEEE 7th Int. Conf. Power Energy, PECon 2018. (2019) 168–173. https://doi.org/10.1109/PECON.2018.8684157.

[18] Y. Tang, Q. Zhang, H. Li, Y. Li, B. Liu, Economic analysis on repurposed EV batteries in a distributed PV system under sharing business models, Energy Procedia. 158 (2019) 4304–4310. https://doi.org/10.1016/j.egypro.2019.01.793.

[19] C.B. Domenech, M. Heleno, Comparing Values of Second Life Batteries to Different Classes of Prosumers in California, (2019) 1–4. https://doi.org/10.1109/greentech.2019.8767122.

[20] X. Han, Y. Liang, Y. Ai, J. Li, Economic evaluation of a PV combined energy storage charging station based on cost estimation of second-use batteries, Energy. 165 (2018) 326–339. https://doi.org/10.1016/j.energy.2018.09.022.

[21] B. Bai, S. Xiong, B. Song, M. Xiaoming, Economic analysis of distributed solar photovoltaics with reused electric vehicle batteries as energy storage systems in China, Renew. Sustain. Energy Rev. 109 (2019) 213–229. https://doi.org/10.1016/j.rser.2019.03.048.

[22] R. Madlener, A. Kirmas, Economic Viability of Second Use Electric Vehicle Batteries for Energy Storage in Residential Applications, Energy Procedia. 105 (2017) 3806–3815. https://doi.org/10.1016/j.egypro.2017.03.890.

[23] S.I. Sun, A.J. Chipperfield, M. Kiaee, R.G.A. Wills, Effects of market dynamics on the time-evolving price of second-life electric vehicle batteries, J. Energy Storage. 19 (2018) 41–51. https://doi.org/10.1016/j.est.2018.06.012.

[24] Z. Song, S. Feng, L. Zhang, Z. Hu, X. Hu, R. Yao, Economy analysis of second-life battery in wind power systems considering battery degradation in dynamic processes: Real case scenarios, Appl. Energy. 251 (2019) 113411. https://doi.org/10.1016/j.apenergy.2019.113411.

[25] T. Alharbi, K. Bhattacharya, M. Kazerani, Planning and Operation of Isolated Microgrids Based on Repurposed Electric Vehicle Batteries, IEEE Trans. Ind. Informatics. 15 (2019) 4319–4331. https://doi.org/10.1109/TII.2019.2895038.

[26] A. Assunção, P.S. Moura, A.T. de Almeida, Technical and economic assessment of the secondary use of repurposed electric vehicle batteries in the residential sector to support solar energy, Appl. Energy. 181 (2016) 120–131. https://doi.org/10.1016/j.apenergy.2016.08.056.

[27] V. V Viswanathan, M. Kintner-Meyer, Second use of transportation batteries: Maximizing the value of batteries for transportation and grid services, IEEE Trans. Veh. Technol. 60 (2011) 2963–2970. https://doi.org/10.1109/TVT.2011.2160378.

[28] A. Berrueta, I. San Martin, J. Pascual, P. Sanchis, A. Ursua, On the requirements of the power converter for second-life lithium-ion batteries, in: 2019 21st Eur. Conf. Power Electron. Appl. EPE 2019 ECCE Eur., Institute of Electrical and Electronics Engineers Inc., 2019. https://doi.org/10.23919/EPE.2019.8915006.

[29] E. Braco, I.S. Martin, P. Sanchis, A. Ursua, Characterization and capacity dispersion of lithiumion second-life batteries from electric vehicles, 2019 IEEE Int. Conf. Environ. Electr. Eng. 2019 IEEE Ind. Commer. Power Syst. Eur. (EEEIC / I&CPS Eur. (2019) 1–6. https://doi.org/10.1109/eeeic.2019.8783547.

[30] Z. Xu, J. Wang, P.D. Lund, Q. Fan, T. Dong, Y. Liang, J. Hong, A novel clustering algorithm for grouping and cascade utilization of retired Li-ion batteries, J. Energy Storage. 29 (2020). https://doi.org/10.1016/j.est.2020.101303.

[31] C. White, B. Thompson, L.G. Swan, Repurposed electric vehicle battery performance in second-life electricity grid frequency regulation service, J. Energy Storage. 28 (2020) 101278. https://doi.org/10.1016/j.est.2020.101278.

[32] S. Tong, T. Fung, M.P. Klein, D.A. Weisbach, J.W. Park, Demonstration of reusing electric vehicle battery for solar energy storage and demand side management, J. Energy Storage. 11 (2017) 200–210. https://doi.org/10.1016/j.est.2017.03.003.

[33] H. Li, M. Alsolami, S. Yang, Y.M. Alsmadi, J. Wang, Lifetime Test Design for Second-Use Electric Vehicle Batteries in Residential Applications, IEEE Trans. Sustain. Energy. 8 (2017) 1736–1746. https://doi.org/10.1109/TSTE.2017.2707565.

[34] Y. Jiang, J. Jiang, C. Zhang, W. Zhang, Y. Gao, N. Li, State of health estimation of second-life LiFePO4 batteries for energy storage applications, J. Clean. Prod. 205 (2018) 754–762. https://doi.org/10.1016/j.jclepro.2018.09.149.

[35] E. Martinez-Laserna, E. Sarasketa-Zabala, I. Villarreal Sarria, D.I. Stroe, M. Swierczynski, A. Warnecke, J.M. Timmermans, S. Goutam, N. Omar, P. Rodriguez, Technical Viability of Battery Second Life: A Study from the Ageing Perspective, IEEE Trans. Ind. Appl. 54 (2018) 2703–2713. https://doi.org/10.1109/TIA.2018.2801262.

[36] T. Waldmann, B.I. Hogg, M. Wohlfahrt-Mehrens, Li plating as unwanted side reaction in commercial Li-ion cells – A review, J. Power Sources. 384 (2018) 107–124. https://doi.org/10.1016/j.jpowsour.2018.02.063.

[37] T.C. Bach, S.F. Schuster, E. Fleder, J. Müller, M.J. Brand, H. Lorrmann, A. Jossen, G. Sextl, Nonlinear aging of cylindrical lithium-ion cells linked to heterogeneous compression, J. Energy Storage. 5 (2016) 212–223. https://doi.org/10.1016/j.est.2016.01.003.

[38] S.F. Schuster, T. Bach, E. Fleder, J. Müller, M. Brand, G. Sextl, A. Jossen, Nonlinear aging characteristics of lithium-ion cells under different operational conditions, J. Energy Storage. 1 (2015) 44–53. https://doi.org/10.1016/j.est.2015.05.003.

[39] J. Wen, Y. Yu, C. Chen, A review on lithium-ion batteries safety issues: Existing problems and possible solutions, Mater. Express. 2 (2012) 197–212. https://doi.org/10.1166/mex.2012.1075.

[40] M. Ecker, N. Nieto, S. Käbitz, J. Schmalstieg, H. Blanke, A. Warnecke, D.U. Sauer, Calendar and cycle life study of Li(NiMnCo)O2-based 18650 lithium-ion batteries, J. Power Sources. 248 (2014) 839–851. https://doi.org/10.1016/j.jpowsour.2013.09.143.

[41] Y. Zhang, Y. Li, Y. Tao, J. Ye, A. Pan, X. Li, Q. Liao, Z. Wang, Performance assessment of retired EV battery modules for echelon use, Energy. 193 (2020) 116555. https://doi.org/10.1016/j.energy.2019.116555.

[42] S.J. Tong, A. Same, M.A. Kootstra, J.W. Park, Off-grid photovoltaic vehicle charge using second life lithium batteries: An experimental and numerical investigation, Appl. Energy. 104 (2013) 740–750. https://doi.org/10.1016/j.apenergy.2012.11.046.

[43] A. Burke, M. Miller, Life cycle testing of lithium batteries for fast charging and second-use applications, 2013 World Electr. Veh. Symp. Exhib. EVS 2014. (2014). https://doi.org/10.1109/EVS.2013.6914962.

[44] T. Le Varlet, O. Schmidt, A. Gambhir, S. Few, I. Staffell, Comparative life cycle assessment of lithium-ion battery chemistries for residential storage, J. Energy Storage. 28 (2020). https://doi.org/10.1016/j.est.2020.101230.

[45] R. van Haaren, M. Morjaria, V. Fthenakis, An energy storage algorithm for ramp rate control of utility scale PV (photovoltaics) plants, Energy. 91 (2015) 894–902. https://doi.org/10.1016/j.energy.2015.08.081.